Dolomite recrystallization revealed by Δ47/U-Pb thermochronometry in the Upper Jurassic Arab Formation, United Arab Emirates

Gasparrini, M.[1], Morad, D.[2], Mangenot, X.[3], Bonifacie, M.[4], Morad, S.[5], Nader, F.H.[2], Gerdes, A.[6]

[1]*Earth Sciences Department, University of Milan, 20133 Milan, Italy*

[2]*IFP Energies nouvelles, 92852 Rueil-Malmaison, France*

[3]*H-Expertise Services, 64370 Pomps, France*

[4]*Université de Paris, Institut de Physique du Globe de Paris, 75005 Paris, France*

[5] *Department of Earth Sciences, Khalifa University, Abu Dhabi, UAE*

[6]*Frankfurt Element und Isotope Research Center (FIERCE), Goethe University Frankfurt, 60438 Frankfurt am Main, Germany*

ABSTRACT

The process of recrystallization affecting dolomitic successions remains a longstanding enigma in carbonate research. Recrystallization influences the accuracy of genetic dolomitization models as well as the prediction of porosity and permeability distribution within dolomitic reservoirs. Here, we investigate early-formed dolomites of the Upper Jurassic Arab Formation reservoir (Arabian Platform), where recrystallization is not easily ascertained based on petrographic and O-C-Sr isotope analyses. Conversely, the application of Δ_{47}/U-Pb thermo-chronometry revealed the occurrence of burial recrystallization over a temperature/time interval of about 45 °C/45 Ma during Early and Late Cretaceous. The process was initially driven by Late Jurassic mixed marine/meteoric waters, which evolved during burial in a closed hydrologic system and remained in thermal equilibrium with the host-rocks. Recrystallization was a stepwise process affecting the succession heterogeneously, so that samples only few meters apart presently record different temperature-time stages of the process and stopped when hydrocarbons migrated into the reservoir. The results illustrate how Δ_{47}/U-Pb thermo-chronometry may provide a novel approach to unravel dolomite recrystallization and to precisely determine timing and physicochemical conditions (temperature, $\delta^{18}O$) of the process. This study therefore paves the ground for a better appraisal of recrystallization in dolomitic reservoirs.

INTRODUCTION

Dolomites that originate early at near-surface conditions are metastable and tend to transform and stabilize via recrystallization. This widely documented diagenetic process does not change the overall rock lithology, though it may cause chemical, crystallographic and textural modifications of early-formed dolomites (e.g. Montañez and Read, 1992; Kupecz and Land, 1994; Machel, 1997). Recrystallization can commence either immediately after dolomitization or during later diagenesis due to interaction with fluids of marine, meteoric or basinal origin (Gregg et al.,1992; Montañez and Read, 1992; Kaczmarek and Sibley, 2014; Ryan et al., 2022). However, preservation of pristine features can be recorded in early dolomites despite the deep burial conditions (Al-Aasm and Packard, 2000). The expression of the dolomite recrystallization process thus remains enigmatic and needs further understanding since recrystallization impacts the accuracy of reconstructed diagenetic models aiming to establish timing, conditions, and mechanism of dolomitization processes.

Despite petrographic and mineralogic clues (e.g. crystal coarsening, increase in non-planar crystal boundaries, stoichiometry and cation ordering, response under cathodoluminescence (CL) or UV-light microscopy, nanotopography type; Kaczmarek and Sibley, 2014; Manche and Kaczmarek, 2021), recrystallization of early dolomites is commonly inferred using isotopic (O, C, Sr) analyses which have been recently complemented by clumped isotope Δ_{47} thermometry (Veillard et al., 2019; Ryan et al. 2022). In parallel, LA-ICPMS U-Pb geochronology has successfully dated early dolomites (Elisha et al., 2020) and opened the possibility to disclose recrystallized dolomites (Montano et al., 2022). However, to our knowledge, no study has combined Δ_{47} thermometry and U-Pb dating (i.e. Δ_{47}/U-Pb thermo-chronometry *sensu* Mangenot et al., 2018) on early-formed dolomites to investigate recrystallization.

The Upper Jurassic Arab Formation (Fm.) of Kimmeridgian to Tithonian age (154-150 Ma) consists of interbedded shallow marine carbonates and evaporites formed on a ramp system under an arid climate and includes a dolomitic succession hosting among the largest hydrocarbon (HC) reserves in the world. Dolomitization is interpreted to occur in the Late Jurassic by syn-depositional to early diagenetic processes, attributable respectively to the evaporative-sabkha and the seepage-reflux systems (e.g. Grötsch et al., 2003; Cantrell et al. 2004; Al Suwaidi et al., 2005; Morad et al., 2012; Marchionda et al. 2018). Here, this succession was investigated using Δ_{47}/U-Pb thermo-chronometry to: (1) demonstrate the occurrence of dolomite recrystallization and place it in a thermochronological framework; (2) shed new light on the spatial/temporal distribution and physicochemical conditions of recrystallization; (3) relate these findings to HC exploration of other dolomitic reservoirs.

MATERIALS AND METHODS

In this study, we investigated Arab Fm. samples from an anticline HC field (Abu Dhabi, UAE) within an intracratonic sedimentary basin of the Arabian Platform (Fig. 1 A-B). Core samples comes from the Arab A-B-C lithostratigraphic members (Fig. 1 C): they formed in supratidal to subtidal environments and consist of high-frequency dolomite-anhydrite shallowing-upward cycles capped by massive anhydrites (Grötsch et al., 2003; Al Suwaidi et al., 2005; Marchionda et al., 2018). The samples come from well A (2834-2850 m) and well C (3303-3366 m), drilled 10 km apart along the anticline crest (Fig. 1 D), i.e. the HC zone.

Aiming to reveal dolomite recrystallization, samples were screened with optical, CL and UV-light petrography (n = 79) and analyzed for O-C isotope compositions (n= 37) and $^{87}Sr/^{86}Sr$ ratios (n = 15). Based on petrographic and geochemical results (Data Repository DR1), a subset of 15 samples was selected for Δ_{47} analyses, including 11 samples that were jointly dated by U-Pb geochronology.

Dolomite Δ_{47} compositions were determined following the protocols summarized in Data Repository DR2. Δ_{47} compositions were converted into temperatures ($T\Delta_{47}$) using the calibration from Bonifacie et al. (2017). The oxygen isotope composition of water ($\delta^{18}O_w$) was calculated from $T\Delta_{47}$ and $\delta^{18}O_{dol}$ simultaneously acquired, by using the oxygen isotope fractionation between dolomite and water from Horita (2014). $\delta^{18}O_{dol}$ and $\delta^{18}O_w$ values are expressed in per mil (‰) relative to the VPDB and the VSMOW standards, respectively. Dolomite U-Pb dating was performed by LA-ICPMS following the method of Ring and Gerdes (2016) and analytical protocols are summarized in Data Repository DR3.

RESULTS

The investigated samples include two non-ferroan and fabric-preserving dolomite types: (1) Dol1 occurs in supratidal to intertidal facies and consists mostly of dolomicrite with fine crystals (< 10 to 30 μm), closely associated to syn-depositional anhydrite beds/nodules; (2) Dol2 occurs in subtidal lagoon facies, and is mainly composed of fine to medium (<10 to 50 μm) and, less commonly, coarse (>50 μm) dolomite crystals, display dolomicrite, planar-s to planar-e textures and is associated to early anhydrite cements. No later dolomite cements were observed. No significant variation in CL response was observed among samples or within single dolomite crystals, whereas UV-light revealed zoned crystals in only a few samples (see Data Repository DR1, Table DR1, Fig. DR1, Table DR4). The $\delta^{18}O_{dol}$ and $\delta^{13}C_{dol}$ values (whole dataset) vary from -5.7 to -1.3 ‰ and from -1.3 to +2.9 ‰, respectively. The $^{87}Sr/^{86}Sr$ ratios range from 0.7070 to 0.7072. The Δ_{47} values indicate temperatures ranging from 42 to 87 °C, corresponding to $\delta^{18}O_w$ between -1.4 and +4.9 ‰ (Fig. 2A, B, Table DR4).

The $^{238}U/^{206}Pb$ and $^{207}Pb/^{206}Pb$ ratios measured on most dolomite samples display concordant Tera-Wasserburg linear regressions (isochrons) with mean squared weighted deviates (MSWD) between 0.59 and 1.90 (Fig. 2C, Fig. DR4_A, Table DR4). Overall, the calculated Concordia lower-intercept U-Pb ages range between 136.5±1.7 and 91.6±7.6 Ma. Single dolomite U-Pb ages are reported in Fig. 2C, Fig. DR4_A and Table DR4.

DOLOMITE RECRYSTALLIZATION REVEALED BY Δ_{47}/U-Pb THERMO-CHRONOMETRY

The studied succession underwent progressive burial from deposition in the Late Jurassic until the onset of a compressional event in the Late Cretaceous which induced faulting and folding together with minor uplift (Johnson et al., 2005). This event was followed by further subsidence during the Paleogene until maximum burial of ~3 km was reached in the Miocene (Morad et al., 2019). Corresponding thermal histories were modelled based on different geothermal gradients between 35 °C/km and 45 °C/km, with the present-day gradient being 38 °C/km (Fig. 3A; see Data Repository DR4). To appraise whether thermal resetting may have modified Δ_{47} compositions, the computed thermal histories were integrated into the Δ_{47} reordering models from Lloyd et al. (2018) and Hemingway and Henkes (2021). The models do not predict any significant Δ_{47} reordering over geological time. Only the first model predicts that dolomite Δ_{47} starts to reorder when assuming a geothermal gradient of 45 °C/km, which is unlikely for the intracratonic basin investigated. Consequently, the measured $T\Delta_{47}$ are expected to reflect the temperatures of initial dolomitization or recrystallization (see Data Repository DR4).

The temperatures/ages determined for the studied dolomites are consistently higher/younger than those expected for Upper Jurassic dolomites formed in near surface environments. These temperatures/ages do not correlate with sample depth, and samples located only a few meters apart may record difference of both several tens of °C and several tens of Ma (Fig. 2, Table DR4). These Δ_{47}/U-Pb data demonstrate that the original dolomites underwent recrystallization and allow constraining timing and physicochemical conditions (temperature, $\delta^{18}O_w$) of the process.

Conventional petrographic approaches to evaluate recrystallization were not straightforward because: (1) no direct relationship was found between dolomite crystal size and temperatures/ages; (2) non-planar textures were not recorded; (3) UV-light response only showed evidence of dissolution/reprecipitation from a few samples (see DR1). This demonstrates that the Δ_{47}/U-Pb thermo-chronometer may be used to complement conventional petrographic indicators for dolomite recrystallization and to provide further insights to interpret this process.

The observed positive covariance between $\delta^{18}O_w$ and $T\Delta_{47}$ (Fig. 2A) indicates that the diagenetic fluid became enriched in ^{18}O with progressive burial. By extrapolating the $\delta^{18}O_w$-$T\Delta_{47}$ regression line towards near-surface temperatures (20-35 °C), at which the original dolomites likely precipitated, it can be inferred that the initial fluids had $\delta^{18}O_w$ between -2 and -4 ‰. These compositions, depleted in ^{18}O compared to the mean seawater, suggest that the original marine evaporative fluids responsible for dolomitization were flushed by meteoric fluids, as observed in other ancient and present sabkha/reflux systems (Spötl and Burns 1991; Sanford and Wood, 2001). These mixed marine/meteoric fluids became progressively enriched in ^{18}O during burial (Fig. 2), due to continuous interaction with the dolomitic host-rocks in a closed hydrologic system with low water renewal (Banner and Hanson, 1990). This scenario agrees with the $^{87}Sr/^{86}Sr$ compositions of the recrystallized dolomites (Fig. 2B) that reflect those of Upper Jurassic seawater carbonates (Veizer et al., 1999; Morad et al., 2018, 2019; see Data Repository DR1).

The Δ_{47} temperatures (42 to 87 °C) and U-Pb ages (136.5 to 91.6 Ma) jointly measured on dolomite samples define eleven temperature-time pairs that overlap, within uncertainties, with the thermal curves of the studied succession that were reconstructed from burial curves and employing paleogeothermal gradients between 35 and 45 °C/km (Fig. 3A; see Data Repository DR4). This finding suggests that the fluids driving the recrystallization process were in thermal equilibrium with the host-rocks. The temperature-time pairs bracket an interval of about 45 °C and 45 Ma, indicating that recrystallization was a stepwise process from Early to Late Cretaceous times, and was not due to one unique fluid-rock interaction event. The results also reveal that recrystallization affected the dolomitic succession heterogeneously such that different portions of the reservoir record different temperature-time stages of the recrystallization process (Fig. 3B). This recrystallization heterogeneity is recorded on the scale of the hand specimens investigated whereas the maximum scale remains uncertain.

CONCLUSIONS AND IMPLICATIONS FOR DOLOMITE RESERVOIR STUDIES

The joint application of Δ_{47} thermometry and U-Pb dating to early-formed dolomites revealed that recrystallization affected the succession heterogeneously and determined timing and some of the physicochemical conditions (temperature, $\delta^{18}O_w$) of the fluids driving the process. Temperature-age datapoints covary and plot on independent thermal history curves suggesting fluids in equilibrium with host-rocks in a closed system. These conclusions would not have been achieved without the application of Δ_{47}/U-Pb thermo-chronometry. Several implications can be derived for the study of dolomitic successions and their potential economic significance:

(1) Dolomite research is widely devoted to the establishment of conceptual genetic models trying to reconstruct timings, diagenetic environments, and fluid delivery mechanisms for dolomitization. However, the common petrographic and geochemical tools used to achieve this aim require that dolomites have not been altered since their initial precipitation (Machel, 1997).

Being able to reveal the occurrence of recrystallization via absolute temperature-time data represents therefore a significant advance in this field.

(2) Recrystallization of early dolomites upon burial is known to affect the textural evolution of dolomites and consequently their porosity and permeability, therefore having an impact on the storage capacities of these worldwide reservoirs (Saller and Handerson, 1998; Nader et al., 2013). The $\delta^{18}O_w$-temperature data from this study agree with those from the Arab Fm. dolomites of the Ghawar field (Swart et al., 2016; Fig. 1 and 2) suggesting that recrystallization occurred in a similar manner (i.e. by mixed marine-meteoric waters in a closed hydraulic system) in reservoirs located hundreds of km apart. It is therefore conceivable to extrapolate the recrystallization scenario proposed here across other reservoirs of the Arabian Platform. Future studies should refine dolomitic reservoir models by also considering the effects of recrystallization on the rock porosity and permeability and its heterogeneous distribution.

(3) One of the concerns in sedimentary basin exploration is to constrain the timing of HC migration. In the study area the onset of the first HC migration started in the Late Cretaceous across several reservoirs (Al Suwaidi et al., 2005; Hollis et al. 2017; Morad et al., 2018) and likely occurred along re-activated strike-slip faults during a compressional tectonic phase (Johnson et al., 2005). Our Δ_{47}/U-Pb data indicate that the recrystallization of dolomites pre-dated this event and was possibly halted by the Late Cretaceous HC migration (Fig. 3). These data support previous hypotheses stating that HC emplacement may inhibit diagenetic processes in carbonate reservoirs (Nielsen et al., 1998; Cox et al., 2010). The assessment of absolute temperatures-ages for the latest stage of dolomite recrystallization could thus potentially be used, in poorly characterized reservoirs, to indirectly constrain HC migration timing.

ACKNOWLEDGMENTS

We thank the Petroleum Institute of Abu Dhabi (PIRC project LTR14012) and IFP Energies nouvelles for funding this survey and ADNOC Sour Gas, ADNOC and Oxy for giving us access to samples, data, and permission to publish. We thank R. Albert for support on U-Pb data processing. FIERCE acknowledges the financial support by the Wilhelm and Else Heraeus Foundation and the DFG.

FIGURE CAPTIONS

Figure 1. A. Arabian Peninsula map with location of the UAE (red area) and of the Ghawar field in Saudi Arabia (grey area) investigated by Swart et al. (2016). **B.** Main hydrocarbon fields (in green) located onshore and offshore Abu Dhabi. The frame includes the studied anticline field. **C.** Field stratigraphy with the Arab A-B-C members located between the Arab D member and the Hith evaporites (modified after Morad et al., 2018). **D.** Location of the sampled wells (A and C) in the anticline field. Isolines indicate relative depth: orange and blue colors represent respectively the highest (crest) and lowest (flanks) elevation of the anticline.

Figure 2. Thermo-chronometry (Δ_{47}/U-Pb) and ^{87}Sr/^{86}Sr data of the Arab Fm. dolomites. **A**: TΔ_{47} *versus* $\delta^{18}O_w$ cross-plot. The square colors refer to the U-Pb ages. Grey squares refer to samples (n=4) not analyzed (NA) with U-Pb geochronology. Data from Arab Fm. dolomites of Ghawar field (Saudi Arabia; Swart et al., 2016) are reported with grey dots. **B:** TΔ_{47} *versus* ^{87}Sr/^{86}Sr cross-plot. The light blue area shows the ^{87}Sr/^{86}Sr of carbonates precipitated from Late Jurassic seawater (Veizer et. al., 1999). **C** and **D**: ^{238}U/^{206}Pb *versus* ^{207}Pb/^{206}Pb Tera-Wasserburg Concordia diagrams and corresponding lower intercept ages for 2 dolomite samples. Data point error ellipses indicate 2σ internal uncertainty of the isotope ratios on “n” analyses. Red lines are the envelopes of the isochrons.

Figure 3. Conceptual scenario of dolomite recrystallization in the Arab Fm. based on Δ_{47}/U-Pb thermo-chronometry. **A.** Thermal histories of Upper Jurassic rocks from the studied field reconstructed by considering different geothermal gradients. The colored squares represent temperature-time pairs measured on dolomites via Δ_{47}/U-Pb thermo-chronometry. Three steps of

the reservoir evolution are illustrated: (1) dolomite formation in Late Jurassic; (2) dolomite recrystallization during Early and Late Cretaceous; (3) begin of HC emplacement in Late Cretaceous. **B.** Schematic well cores illustrate the stepwise recrystallization process that affected heterogeneously the original dolomites and pre-dated hydrocarbon (HC) charging.

[1] GSA Data Repository includes: dolomite petrography and O-C-Sr isotope geochemistry (Table DR1, Figure DR1_A, Figure DR1_B, Figure DR1_C), Δ_{47} and U-Pb methods, further Δ_{47}/U-Pb data and discussion (Table DR4, Figure DR4_A, Figure DR4_B), U-Pb raw data (Table DR5). It is available online or on request from editing@geosociety.org

REFERENCES CITED

1) Al-Aasm, I.S., Packard, J.J., 2000. Stabilization of early-formed dolomite: a tale of divergence from two Mississippian dolomites. Sedimentary Geology, 131, 97-108. DOI:10.1016/S0037-0738(99)00132-3

2) Al Suwaidi, A.S., El Hami, M., Hagiwara, H., Aziz, S.K., Al Habshi, A.R., 2011. Carbonates and evaporites of the Upper Jurassic Arab Formation, Abu Dhabi: a petroleum exploration challenge. In: Kendall, C.G.S.C., Alsharhan, A.S. (eds) Quaternary carbonate and evaporite sedimentary facies and their ancient analogues: a tribute to Douglas James Shearman, 43. International Association of Sedimentologists, 421–430. DOI: 10.1002/9781444392326.ch19

3) Banner, J. L., Hanson, G.N., Meyers, W.J., 1988. Water-rock interaction history of regionally extensive dolomites of the Burlington-Keokuk Formation (Mississippian): isotopic evidence. In: Shukla, V., Baker, P. (eds), Sedimentology and geochemistry of dolostones. SEPM Special Publication, 43, 97–113. DOI:10.2110/pec.88.43.0097

4) Bonifacie, M., Calmels, D., Eiler, J.M., Horita, J., Chaduteau, C., Vasconcelos, C., Agrinier, P., Katz, A., Passey, B.H., Ferry, J.M., Bourand, J.J., 2017. Experimental calibration of the dolomite clumped isotope thermometer from 25 to 350°C, and implications for the temperature estimates for all (Ca, Mg, Fe) CO_3 carbonates digested at high temperature. Geochimica et Cosmochimica Acta, 200, 255-279. DOI:10.1016/j.gca.2016.11.028

5) Cantrell, D. Swart, P., Hagerty, R., 2004, Genesis and characterization of dolomite Arab-D reservoir, Ghawar Field, Saudi Arabia: Geo-Arabia, v. 9, p. 11–36.

6) Cox, P.A., Wood, R.A., Dickson, J.A.D., Al Rougha, H.B., Shebl, H., Corbett, P.W.M., 2010. Dynamics of cementation in response to oil charge: evidence from a Cretaceous carbonate field, UAE. Sedimentary Geology, 228, 246–254. DOI:10.1016/j.sedgeo.2010.04.016

7) Elisha, B., Nuriel, P., Kylander-Clark,A., Weinberger, R., 2020. Towards in-situ U–Pb dating of dolomites. Geochronology, 3(1): 337-349. DOI:10.5194/gchron-2020-19, 2020

8) Gregg, J.M., Howard, S.A., Mazzullo, S.J., 1992. Early diagenetic recrystallization of Holocene (<3000 years old) peritidal dolomites, Ambergris Cay, Belize. Sedimentology, 39, 143-159. DOI:10.1111/j.1365-3091.1992.tb01027.x

9) Grötsch, J., Suwaina, O., Ajlani, G., Taher, A., El-Khassawneh, R., Lokier, S., Coy, G., Van der Weerd, E., Masalmeh, S., Van Dorp, J., 2003. The Arab Formation in central Abu Dhabi: 3-D reservoir architecture and static and dynamic modeling. GeoArabia 8 (no. 1), 47–86.

10) Hemingway, J.D, Henkes, G.A., 2021. A disordered kinetic model for clumped isotope bond reordering in carbonates. Earth and Planetary Science Letters, 566, 116962. DOI: 10.1016/j.epsl.2021.116962

11) Hollis, C., Lawrence, D.A., de Perière, M.D., Al Darmaki, F., 2017. Controls on porosity preservation within a Jurassic oolitic reservoir complex. UAE. Marine and Petroleum Geology, 88, 888–906. DOI:10.1016/j.marpetgeo.2017.09.015

12) Horita, J., 2014. Oxygen and carbon isotope fractionation in the system dolomite–water–CO_2 to elevated temperatures. Geochimica et Cosmochimica Acta, 129, 111– 24. DOI:10.1016/j.gca.2013.12.027

13) Johnson, C.A., Hauge, T., Al-Menhali, S., Bin Sumaidaa, S., Sabin, B., West, B., 2005. Structural styles and tectonic evolution of onshore and offshore Abu Dhabi, UAE. Society of Petroleum Engineers. International Petroleum Technology Conference, Doha, Qatar, November 2005. DOI: 10.2523/IPTC-10646-MS

14) Kaczmarek, S.E., Sibley, D.F., 2014. Direct physical evidence of dolomite recrystallization. Sedimentology, 61, 1862-1882. DOI:10.1111/sed.12119

15) Kupecz, J.A., Land, L.S., 1994. Progressive recrystallization and stabilization of early-stage dolomite: Lower Ordovician Ellenburger Group, West Texas. In: Purser, B., Tucker, M., Zenger, D. (eds), Dolomites: a volume in honour of Dolomieu. IAS Special Publication, 255-279. DOI:10.1002/9781444304077.ch15

16) Lloyd, M.K., Ryb, U., Eiler, J.M., 2018. Experimental calibration of clumped isotope reordering in dolomite. Geochimica et Cosmochimica Acta, 242, 1-20. DOI:10.1016/j.gca.2018.08.036

17) Machel, H.G., 1997. Recrystallization *versus* neomorphism, and the concept of significant recrystallization in dolomite research. Sedimentary Geology, 113, 161-168. DOI:10.1016/S0037-0738(97)00078-X

18) Manche, C.J., Kackzmarek, S.E., 2021. A global study of dolomite stoichiometry and cation ordering through the Phanerzoic. J. Sediment. Res., 91, 520–546. DOI: 10.2110/jsr.2020.204

19) Mangenot, X., Gasparrini, M., Gerdes, A., Bonifacie, M., & Rouchon, V., 2018. An emerging thermo-chronometer for carbonate bearing-rocks: Δ_{47}/(U-Pb). Geology, 46 (12), 1067-1070. DOI:10.1130/G45196.1

20) Marchionda, E., Deschamps, R., Cobianchi, M., Nader, F.H., Di Giulio, A., Morad, D.J., Al Darmaki, F., Ceriani, A., 2018. Field-scale depositional evolution of the Upper Jurassic Arab Formation (onshore Abu Dhabi, UAE). Mar. Petrol. Geol. 89, 350–369. DOI: 10.1016/j.marpetgeo.2017.10.006

21) Montañez, I.P., Read, J.F., 1992. Fluid-rock interaction history during stabilization of early dolomites, Upper Knox Group (Lower Ordovician), US Appalachians. Journal of Sedimentary Petrology, 62: 753-778. DOI:10.1306/D42679D3-2B26-11D7-8648000102C1865D

22) Morad, S., Al-Aasm, I.S., Nader, F.H., Ceriani, A., Gasparrini, M., Mansurbeg, H., 2012. Impact of diagenesis on the spatial and temporal distribution of reservoir quality in the Jurassic Arab D and C members, offshore Abu Dhabi oilfield, United Arab Emirates. GeoArabia, 17(3), 17-56.

23) Morad, D., Nader, F.H., Gasparrini, M., Morad, S., Rossi, C., Marchionda, E., Al Darmaki, F., Martines, M., Hellevang, H., 2018. Comparison of the diagenetic and reservoir quality evolution between the anticline crest and flank of an Upper Jurassic carbonate gas reservoir, Abu Dhabi, United Arab Emirates. Sediment. Geol. 367, 96–113. DOI:10.1016/j.sedgeo.2018.02.008

24) Morad, D., Nader, F.H., Morad, S., Rossi, C., Gasparrini, M., Al Darmaki, F., Hellevang, H., 2019. Limited thermochemical sulfate reduction (TSR) in hot sour gas carbonate - anhydritic reservoirs of the Upper Jurassic Arab Formation, United Arab Emirates. Marine and Petroleum Geology, 106, 30-41. DOI:10.1016/j.marpetgeo.2019.04.023

25) Montano, D., Gasparrini, M., Rohais, S., Albert, R., Gerdes, A., 2022. Depositional age models in lacustrine systems from zircon and carbonate U-Pb geochronology. Sedimentology, 69, 2507–2534, DOI:10.1111/sed.13000

26) Nader, F.H., De Boever, E., Gasparrini, M., Liberati, M., Dumont, C., Ceriani, M., Morad, S., Lerat, O., Doligez, B., 2013. Quantification of diagenesis impacts on reservoir properties of the Jurassic Arab D and C members (offshore, U.A.E). Geofluids, 13(2): 204-220. DOI: 10.1111/gfl.12022

27) Neilson, J.E., Oxtoby, N.H., Simmons, M.D., Simpson, I.R., Fortunatova, N.K., 1998. The relationship between petroleum emplacement and carbonate reservoir quality: examples from Abu Dhabi and the Amu Darya Basin. Marine and Petroleum Geology, 15, 57–72. DOI:10.1016/S0264-8172(97)00033-0

28) Ring, U., Gerdes, A., 2016. Kinematics of the Alpenrhein-Bodensee graben system in the Central Alps: Oligocene/Miocene transtension due to formation of the Western Alps arc. Tectonics, 35, 1367–1391. DOI:10.1002/2015TC004085

29) Ryan, B.H., Kaczmarek, S.E., Rivers, J.M., Manche, C.J., 2022. Extensive recrystallization of Cenozoic dolomite during shallow burial: A case study from the Palaeocene–Eocene Umm er Radhuma formation and a global meta-analysis. Sedimentology, 69(5), 2053-2079. DOI: 10.1111/sed.12982

30) Saller, A.H., Handerson, N., 1998. Distribution of porosity and permeability in platform dolomites: insight from the Permian of West Texas. AAPG Bulletin, 82, 8, 1528-1550. DOI:10.1306/090800850530

31) Sanford, W.E., Wood, W.W., 2001. Hydrology of the coastal sabkhas of Abu Dhabi, United Arab Emirates. Hydrogeology Journal, 9, 358–366. DOI: 10.1007/s100400100137

32) Spötl. C., Burns, S.J., 1991. Formation of ^{18}O-depleted dolomite within a marine evaporitic sequence, Triassic Reichenhall Formation, Austria. Sedimentology 38 (6), 1041–1057. DOI:10.1111/j.1365-3091.1991.tb00370.x

33) Swart, P.K., Cantrell, D.L., Arienzo, M.M., Murray, S.T., 2016. Evidence for high temperature and ^{18}O-enriched fluids in the Arab-D of the Ghawar Field, Saudi Arabia. Sedimentology, 63, 1739-1752. DOI:10.1111/sed.12286:

34) Veillard, C.M.A., John, C.M., Krevor, S., Najorka, J., 2019. Rock-buffered recrystallization of Marion Plateau dolomites at low temperature evidenced by clumped isotope thermometry and X-ray diffraction analysis. Geochimica et Cosmochimica Acta, 252, 190-212. DOI : 10.1016/j.gca.2019.02.012

35) Veizer, J., Ala, D., Azmy, K., Bruckschen, P., Buhl, D., Bruhn, F., Garden, G.A.F., Diener, A., Ebneth, S., Godderis, Y., Japer, T., Korte, C., Pawellek, F., Podlaha., O.G. Strauss, H., 1999. ^{87}Sr/^{86}Sr, δ^{13}C and δ^{18}O evolution of Phanerozoic seawater. Chemical Geology, 161, 59–88. DOI:10.1016/S0009-2541(99)00081-9

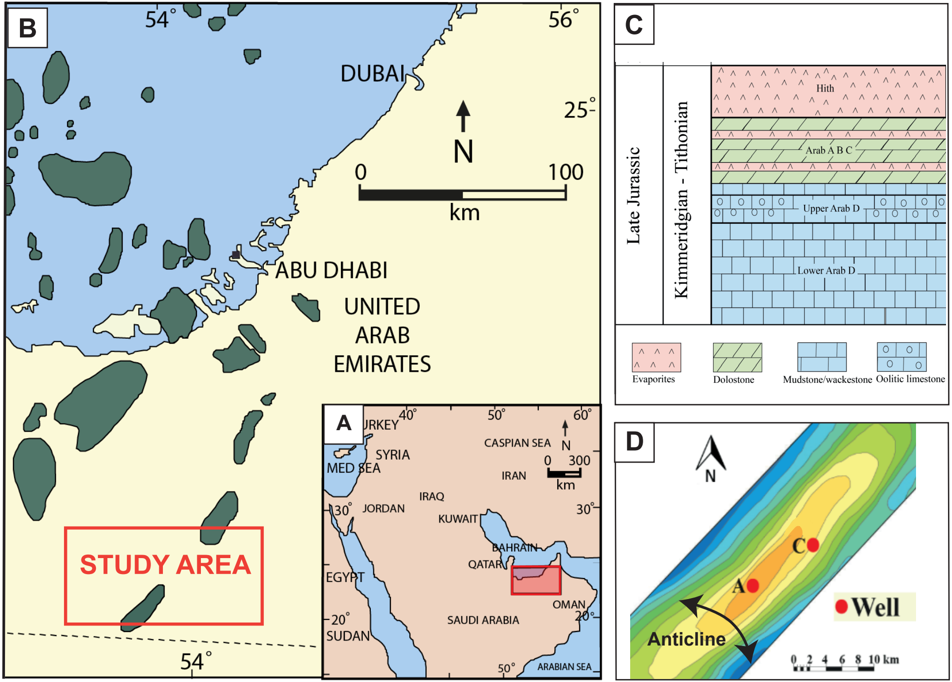
B
54°
56°
DUBAI
25°
N
0
100
km
ABU DHABI
UNITED
ARAB
EMIRATES
STUDY AREA
54°
A
URKEY
40°
50°
60°
CASPIAN SEA
N
0
300
km
SYRIA
MED SEA
IRAN
IRAQ
30°
JORDAN
KUWAIT
30°
BAHRAIN
QATAR
EGYPT
OMAN
20°
20°
SAUDI ARABIA
SUDAN
50°
ARABIAN SEA
C
Late Jurassic
Kimmeridgian - Tithonian
Hith
Arab A B C
Upper Arab D
Lower Arab D
Evaporites
Dolostone
Mudstone/wackestone
Oolitic limestone
D
N
C
A
Well
Anticline
0 2 4 6 8 10 km

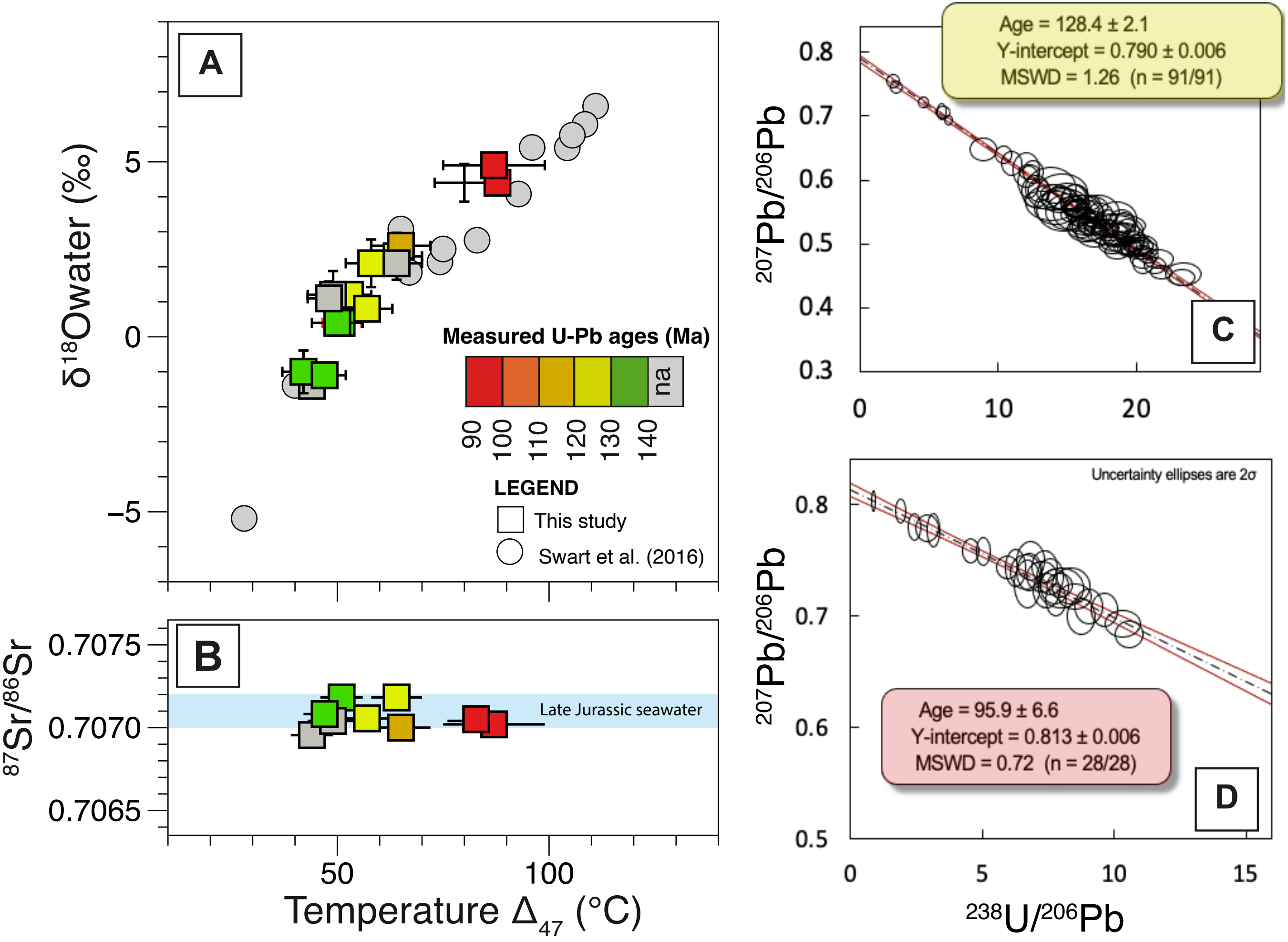
A
B
C
D
δ18Owater (‰)
5
0
−5
Measured U-Pb ages (Ma)
na
90
100
110
120
130
140
LEGEND
This study
Swart et al. (2016)
87Sr/86Sr
0.7075
0.7070
0.7065
Late Jurassic seawater
50
100
Temperature Δ47 (°C)
Age = 128.4 ± 2.1
Y-intercept = 0.790 ± 0.006
MSWD = 1.26 (n = 91/91)
207Pb/206Pb
0.8
0.7
0.6
0.5
0.4
0.3
0
10
20
Uncertainty ellipses are 2σ
Age = 95.9 ± 6.6
Y-intercept = 0.813 ± 0.006
MSWD = 0.72 (n = 28/28)
207Pb/206Pb
0.8
0.7
0.6
0.5
0
5
10
15
238U/206Pb

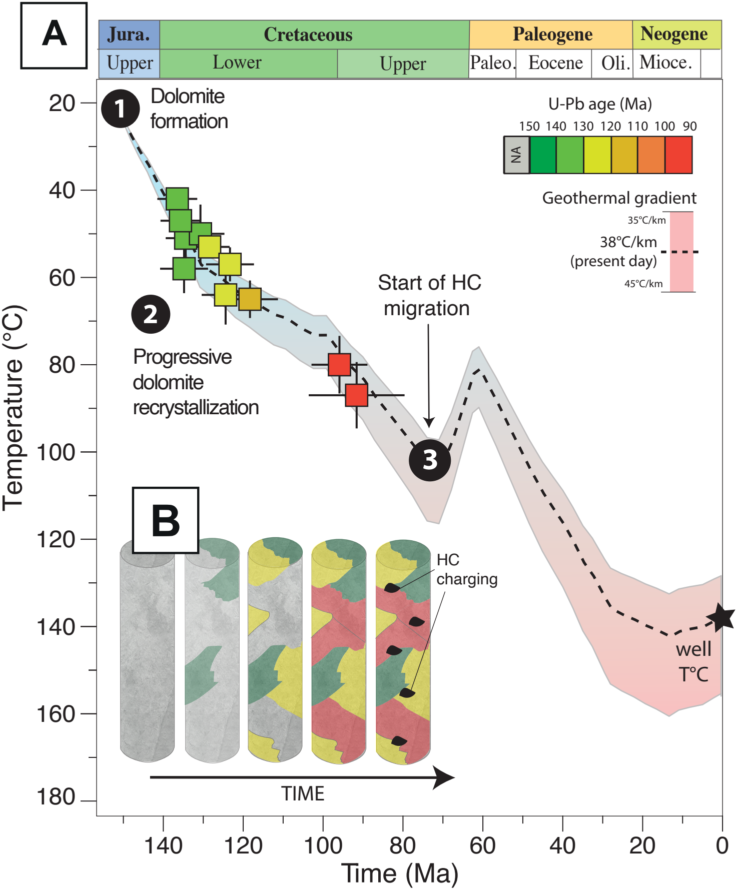
A
Jura.
Cretaceous
Paleogene
Neogene
Upper
Lower
Upper
Paleo.
Eocene
Oli.
Mioce.
1 Dolomite formation
U-Pb age (Ma)
150 140 130 120 110 100 90
NA
Geothermal gradient
35°C/km
38°C/km (present day)
45°C/km
Start of HC migration
2
Progressive dolomite recrystallization
3
B
HC charging
well T°C
TIME
Temperature (°C)
20
40
60
80
100
120
140
160
180
140
120
100
80
60
40
20
0
Time (Ma)